Method for Calculating the Unsteady Flow of an Elliptical Circulation-Control Airfoil

Mao Sun* and Wei Wang†
Beijing Institute of Aeronautics and Astronautics, Beijing, China

A numerical method is developed to study the unsteady aerodynamics of an elliptical airfoil in two-dimensional incompressible flow. In this method, it is assumed that the separation positions of the wall jet on the upper surface and the boundary layer on the lower surface of the airfoil can be determined by solving the quasisteady boundary-layer equations; the discrete vortex model is used to model the wake, and the potential flow is calculated by conformal mapping technique. Results are presented and discussed for a number of cases that illustrate relevant characteristics of the unsteady flow of circulation-control airfoils.

Nomenclature

a = semimajor axis of an ellipse
b = semiminor axis of an ellipse
C_m = pitching-moment coefficient (about $0.5c$), moment/qc^2
C_p = pressure coefficient, perturbation pressure/qc
C_y = lift coefficient, lift/qc
C_μ = blowing-momentum coefficient, blowing-momentum flux/q
c = airfoil chord length
i = $\sqrt{-1}$
K = strength of free vortex
k = reduced frequency, $\omega c/2u_\infty$
p = pressure
q = dynamic pressure, $\rho u_\infty^2/2$
r = polar coordinate in circle plane
t = time
$U + iV$ = velocity of airfoil
$u + iv$ = absolute velocity of fluid
u_e = flow speed at boundary-layer edge
u_∞ = freestream speed
$\bar{v}_R$ = relative velocity of fluid
w = complex potential
x,y = rectangular coordinates in physical plane
x_p = airfoil pitching-axis location
z = complex coordinate in physical plane
α = angle of attack
$\dot{\alpha}$ = angular velocity
ζ = complex coordinate in circle plane
θ = polar coordinate in circle plane
θ_{fs} = forward stagnation angle
θ_s = separation angle in Fig. 4
θ_{10} = upper-surface separation angle
θ_{20} = lower-surface separation angle
ξ,η = rectangular coordinates in circle plane
ρ = density
ϕ = real part of $w(z)$
ω = oscillation frequency

Superscript

$(\bar{\cdot})$ = complex conjugate

Introduction

IN a circulation-control airfoil (Fig. 1), air is injected tangentially from a slot near its round trailing edge to delay the boundary-layer separation, as well as to increase the circulation around the airfoil. The circulation-control airfoil can achieve a high lift coefficient at a moderate momentum coefficient of the blowing jet,[1] and can be effectively applied to V/STOL aircraft and advanced rotorcraft.[2,3] Much effort has been made to determine experimentally and theoretically the aerodynamic characteristics of circulation-control airfoils at steady-state conditions.[1-5] Current methods can predict the aerodynamic forces and moments with reasonable accuracy.[4,5] But in practical application, the circulation-control airfoil often operates in an unsteady aerodynamic environment. For instance, as the airfoil is applied to a helicopter rotor in forward flight, the velocity, angle of attack, and blowing rate of the airfoil vary periodically with time. It is necessary to study the unsteady aerodynamic characteristics of such airfoils and develop a prediction method. At this time, data on unsteady characteristics of circulation-control airfoils are very limited. Recently, Raghaven et al.[6] have developed a numerical method to study the unsteady aerodynamics of elliptic circulation-control airfoils with oscillation in freestream speeds and in jet blowing rates. In their method, the unsteady outer flow (flow outside boundary layer and wake regions) is not calculated but is assumed to be a quasisteady variation of the steady flow. This approximation neglects the effects of unsteady wake and the effect of the movement of boundary-layer separation points on the outer flow.

The present paper describes a method for studying the unsteady flow about an elliptical circulation-control airfoil performing translating and pitching oscillations with moderate amplitude and frequency. The effect of the periodical variation of the jet blowing rate is included in the method. The flow considered is incompressible and two-dimensional. In this method, the flowfield is divided into potential flow, boundary layer (including wall jet), and wake (Fig. 1). Boundary-layer theory is used to determine the separation points on the upper and lower surfaces of the airfoil, a discrete vortex model is

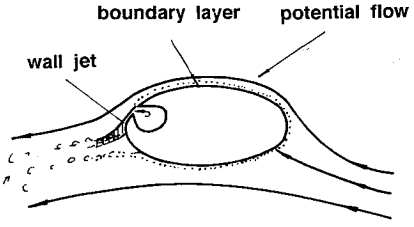

Fig. 1 Circulation-control airfoil.

Received March 27, 1988; revision received April 13, 1989.

*Associate Professor, Department of Applied Mechanics and Aircraft Design.
†Graduate Research Assistant, Department of Applied Mechanics and Aircraft Design.

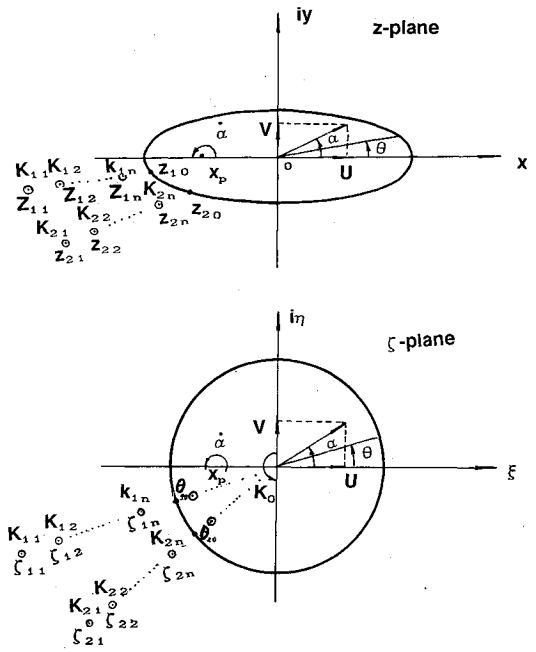

Fig. 2 Mapping between the physical and transformed plane.

used to model the wake by introducing nascent vortices near the separation points at each time step, and the potential flow is calculated by a conformal mapping technique.

Description of the Method

Potential Flow and the Wake

Consider that the airfoil translates with velocity $U + iV$ and rotates about point x_p with angular velocity $\dot{\alpha}$ in an unbounded incompressible fluid at rest at infinity (Fig. 2). The z frame is fixed on the airfoil. Continuous vortex sheets will be shed into the wake from the upper and lower separation points z_{10} and z_{20}, which are known from the boundary-layer calculation described in next section. In our method, the vortex sheets are approximated by discrete vortices and at each time step two nascent vortices are introduced near the separation points. At the nth time step, there are $2n$ vortices of strength K_{11}, $K_{12}, \cdots, K_{1n}, K_{21}, K_{22}, \cdots, K_{2n}$, located at $z_{11}, z_{12}, \cdots, z_{1n}, z_{21}, z_{22}, \cdots, z_{2n}$. As shown in Fig. 2, the transformation

$$z = \frac{a+b}{2}\zeta + \frac{a-b}{2}\frac{1}{\zeta} \tag{1}$$

maps a circle of unit radius in the ζ plane into an elliptical airfoil in the physical $z(x+iy)$ plane. A discrete vortex of circulation K_{ml} at a position z_{ml} outside of the airfoil is transformed according to Eq. (1) into a vortex of the same strength at ζ_{ml} outside the circle and its corresponding image at $1/\bar{\zeta}_{ml}$. The complex potential function in the ζ plane, following Ref. (7), is

$$w(\zeta) = -(bU + iaV - ia\dot{\alpha}x_p)1/\zeta - i\dot{\alpha}\frac{a^2-b^2}{4}\frac{1}{\zeta^2} - iK_0 \ell n\zeta - i\sum_{j=1}^{n}\left(K_{1j}\ell n\frac{\zeta-\zeta_1}{\zeta-1/\bar{\zeta}_{1j}} + K_{2j}\ell n\frac{\zeta-\zeta_{2j}}{\zeta-1/\bar{\zeta}_{2j}}\right) \tag{2}$$

where K_0 is the circulation around the airfoil when it is in steady motion. The complex velocity in the z plane is

$$\frac{dw}{dz} = \frac{dw}{d\zeta}\frac{d\zeta}{dz} \tag{3}$$

where

$$\frac{d\zeta}{dz} = \frac{2\zeta^2}{(a+b)\zeta^2 - (a-b)}$$

The rate at which the vorticity is shed into the wake from a separation point may be closely approximated by[8]

$$\frac{\partial K}{\partial t} = \frac{1}{4\pi}u_{e,j}^2 \tag{4}$$

where $u_{e,j}$ is the speed of the outer flow at the separation point (looking from the moving frame). Thus, the strengths of the nascent vortices are given by

$$K_{1n} = \frac{\Delta t}{4\pi}u_{e,1}^2, \qquad K_{2n} = \frac{\Delta t}{4\pi}u_{e,2}^2 \tag{5}$$

where Δt is the time increment, and $u_{e,1}$ and $u_{e,2}$ are the outer flow speeds at the upper separation point z_{10} and lower separation point z_{20}, respectively. The nascent vortices are introduced into the flow at

$$\zeta_{1n} = r_1 e^{1\theta_{10}}, \qquad \zeta_{2n} = r_2 e^{1\theta_{20}} \tag{6}$$

with the requirement that the no-slip condition is satisfied at z_{10} and z_{20}, i.e.,

$$\left(\frac{dw}{dz}\right)_{z_{10}} - \{(U - \dot{\alpha}y_{10}) + i[\dot{\alpha}(x_{10} - x_p) + V]\} = 0 \tag{7a}$$

$$\left(\frac{dw}{dz}\right)_{z_{20}} - \{(U - \dot{\alpha}y_{20}) + i[\dot{\alpha}(x_{20} - x_p) + V]\} = 0 \tag{7b}$$

Equations (7) are solved for r_1 and r_2, and thus ζ_{1n} and ζ_{2n} are determined. These vortices will later move at the local fluid velocity without changing their circulations.

The complex velocity of all discrete vortices in the physical plane, e.g., the vortex at z_{1l} of strenth K_{1l}, is derived as

$$(u - iv)_{z_{1l}} = \left\{(bU + iaV - ia\dot{\alpha}x_p)\cdot\frac{1}{\zeta_{1l}^2} + i\dot{\alpha}\frac{a^2+b^2}{2\zeta_{1l}^3} - iK_0\frac{1}{\zeta_{1l}} - i\sum_{j\neq 1}^{n}K_{1j}\frac{1}{\zeta_{1l}-\zeta_{1j}} + i\sum_{j=1}^{n}\left[K_{1j}\frac{1}{\zeta_{1j}-1/\bar{\zeta}_{1j}} - K_{2j}\left(\frac{1}{\zeta_{1l}-\zeta_{2j}} - \frac{1}{\zeta_{1l}-1/\bar{\zeta}_{2j}}\right)\right]\right\}\cdot\frac{2\zeta_{1l}^2}{(a+b)\zeta_{1l}^2 - (a-b)} + \frac{i2K_{1l}(a-b)\zeta_{1l}}{[(a+b)\zeta_{1l}^2 - (a-b)]^2} \tag{8}$$

At time t_{n-1}, the mlth vortex in the z plane is located at $z_{ml}^{(n-1)}$. As time is advanced by an increment Δt to t_n, the vortex will have a displacement of

$$\Delta z_{ml} = \int_{t_{n-1}}^{t_n}(u + iv)_{z_{ml}}\,dt \tag{9}$$

In the same time interval, the airfoil and z frame will translate in the x and y directions by distances of

$$\Delta x = \int_{t_{n-1}}^{t_n}U dt, \qquad \Delta y = \int_{t_{n-1}}^{t_n}V dt \tag{10}$$

respectively, and rotate about point x_p by an angle of

$$\beta = \int_{t_{n-1}}^{t_n}\dot{\alpha}\,dt \tag{11}$$

The origin of the z frame will move to (as viewed from the z frame at time t_{n-1})

$$z^* = \Delta x + x_p(1 - \cos\beta) + i(\Delta y - x_p\sin\beta) \tag{12}$$

Therefore, at time t_n, the position of mlth vortex $z_{ml}^{(n)}$ in terms of its former location $z_{ml}^{(n-1)}$ is

$$z_{ml}^{(n)} = [(z_{ml}^{(n-1)} + \Delta z_{ml}) - z^*]e^{i\beta} \tag{13}$$

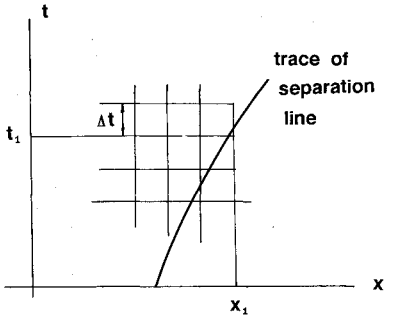

Fig. 3 Finite-difference grid pattern in the x-t plane in the case where separation moves rearward with time.

In calculating $z_{ml}^{(n)}$ by Eqs. (9–13), a two-step predictor-corrector procedure is used.

At time t_n, the fluid velocity at a point on the airfoil surface, (x_s,y_s), as viewed in the moving frame, is

$$\bar{v}_R = \left(\frac{\overline{dw}}{dz}\right)_{(x_s,y_s)} - \bar{v}_A \tag{14}$$

where

$$\bar{v}_A = (U - \dot{\alpha}y_s) + i[V + \dot{\alpha}(x_s - x_p)] \tag{15}$$

is the velocity of the same point regarded as fixed to the moving frame. The pressure on the surface of the airfoil is given by the unsteady Bernoulli's equation in the moving frame[7]:

$$\frac{p}{\rho} = C(t) - \frac{1}{2}v_R^2 + \frac{1}{2}v_A^2 - \frac{\partial\phi}{\partial t} \tag{16}$$

where

$$\phi = \text{real}[w(z)] \tag{17}$$

and $C(t)$ is a function of time. From Eq. (2), we have

$$\frac{\partial\phi(x_s,y_s,t)}{\partial t} = \frac{\partial\phi(1,\theta,t)}{\partial t} = -b\frac{\partial U}{\partial t}\cos\theta - a\frac{\partial V}{\partial t}\sin\theta + a\frac{\partial\dot{\alpha}}{\partial t}x_p\sin\theta - \frac{(a^2-b^2)}{4}\frac{\partial\dot{\alpha}}{\partial t}\sin\theta - \frac{\partial}{\partial t}\,\text{real} \times\left[i\sum_{j=1}^{n}\left(K_{1j}\frac{e^{i\theta}-\zeta_{1j}}{e^{i\theta}-1/\bar{\zeta}_{1j}} + K_{2j}\frac{e^{i\theta}-\zeta_{2j}}{e^{i\theta}-1/\bar{\zeta}_{2j}}\right)\right] \tag{18}$$

$\bar{v}_R$ in Eq. (14) and p in Eq. (16) provide outer boundary conditions for the boundary-layer calculation. The forces and moments acting on the airfoil at any time are obtained by integrating Eq. (16) around the airfoil surface.

When the distance between two vortices in the wake becomes too small, erratic vortex motion occurs due to the unrealistically large velocity near the center of the idealized vortex. To eliminate this erratic motion of the vortices, the two vortices are combined into one situated at their centroid position, whose circulation is the sum of the two individual strengths. To reduce computation time, the vortices whose distances from the airfoil trailing edge is larger than eight times the airfoil chord length are assumed to be at rest with respect to the still air at infinity.

Determination of Separation Points

When the circulation-control airfoil is performing translating and pitching oscillation, and/or the jet blowing rate is varying periodically, the separation points of the wall jet on the upper surface and the boundary layer on the lower surface of the airfoil will oscillate about their mean positions, respectively. It is not yet possible to determine the oscillating separation points through solving the unsteady boundary-layer equations numerically.[9] This is because when the separation point is moving rearward along the body, the domain of integration is always expanding. If a solution is to be obtained at a time $t_1 + \Delta t$ (Fig. 3) at an x station close to separation, say x_1, information would be required for the same x station at the previous time t_1; the point (x_1,t_1) lies beyond the separation point at time t_1 and thus no information is available to make the required calculations. In previous works in which determination of oscillating separation point is needed, an approximate method had to be used. Sarpkaya and Schoaff,[10] in studying the unsteady flow around a circular cylinder, assumed the boundary-layer flow to be quasisteady and used the Pohlhausen method to determine separation points. Stansby and Dixon[11] based their predictions of separation points of circular cylinders on experimental data.

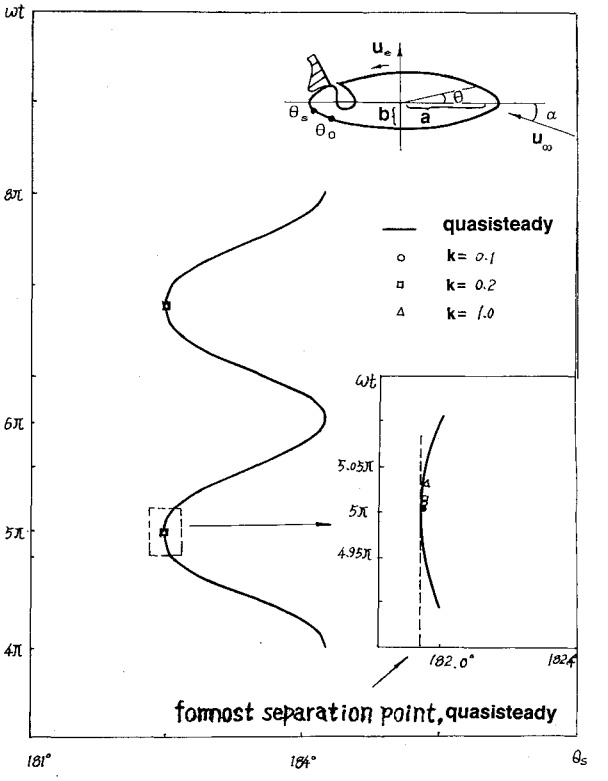

Fig. 4 Upper separation-point variation with time as the outer flow varies sinusoidally with time ($b/a = 0.2$; $u_\infty = 100$ m/s; $\epsilon_1 = 0.1$; $\alpha = 0$ deg; $\theta_0 = 195$ deg; and $C_\mu = 0.005$).

In the present work, we first study the response of unsteady separation of the wall jet on a circulation-control airfoil to prescribed periodically varying outer flows and jet blowing rates. Based on the results of this study, some approximations are made on the boundary layer and the wall-jet calculations so that the oscillating separation points can be determined.

Consider the unsteady separation of a wall jet on the upper surface of an elliptical circulation-control airfoil (Fig. 4). The outer flow was assumed as

$$u_e = u_\infty(1 - \epsilon_1\cos\omega t)\frac{(a+b)[\sin(\theta+\alpha) - \sin(\theta_0+\alpha)]}{[b^2 + (a^2-b^2)\sin^2\theta]^{1/2}} \tag{19}$$

where ϵ_1 is a constant and ω is the frequency of outer flow oscillation. Figure 4 gives the definitions of other symbols in Eq. (19). Letting $\epsilon_1 = 0$, Eq. (19) becomes the surface velocity distribution of an elliptical airfoil with rear stagnation point at θ_0. The blowing rate of the wall jet was given by the momentum coefficient C_μ.

The development of the wall jet is calculated by solving the unsteady Reynolds-averaged boundary-layer equations with

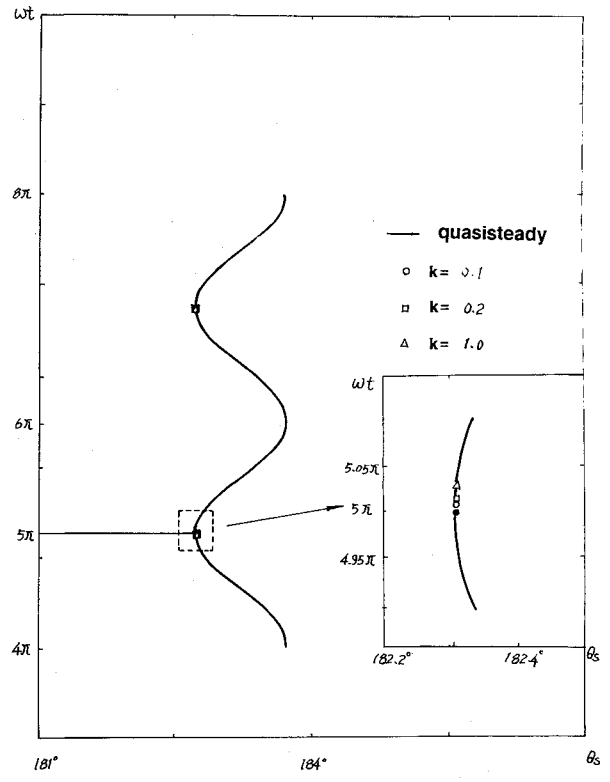

Fig. 5 Upper separation-point variation with time as the wall jet flowing rate varies sinusoidally with time ($b/a = 0.2$; $u_\infty = 100$ m/s; $\epsilon_1 = 0$; $\epsilon_2 = 0.1$; $C_\mu = 0.055$; $\alpha = 0$ deg; and $\theta_0 = 195$ deg).

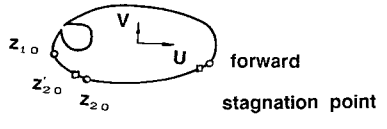

Fig. 6 Calculation process of the steady flow.

Keller and Cebeci's finite-difference method (Ref. 12, p. 344). Dvorak's[13] eddy-viscosity model for the Reynolds stress of a wall jet on a round surface is used in the present work. The calculation starts from the jet exit. Patel[14] has shown from momentum considerations that the effect of the boundary layer upstream of the slot on the wall-jet development is of second-order importance, so that its influence may be reasonably neglected under most conditions in analyzing the jet development. Bradshaw and Gee[15] demonstrated experimentally that the influence of even a very thick boundary layer does not appreciably affect the behavior of the wall jet provided that the jet discharge is substantially greater than the local external velocity at the slot exit, which is the case in a circulation-control airfoil. In view of this information, the existence of the upstream boundary layer is ignored in the present work.

The separation was identified by the singularity criterion of unsteady separation. Only the foremost position of the oscillating separation point (see Fig. 4) can be calculated for reasons stated previously. The separation point of the wall jet is also calculated by the quasi-steady-state method (i.e., solving steady boundary-layer equations under instantaneous outer flow conditions). By comparing the unsteady and quasisteady-state results for the foremost position of the separation point, one can see the dynamic properties of the separation movement.

Figure 4 shows the time variation of the separation position of the wall jet when the jet blowing rate is kept constant and the outer flow is varying with time according to Eq. (19) (for the unsteady case, only the foremost position of the separation point is shown in the figure). It is seen that when the reduced frequency $k < 0.2$, the foremost position of the separation point is almost identical to that calculated by the quasi-steady-state method. When $k = 1.0$, the phase difference between the unsteady and quasi-steady-state calculations is only about 3 deg. Figure 5 shows the variation of the separation position of the wall jet with time when the jet blowing rate is varying as $C_\mu = C_{\mu_0}(1 - \epsilon_2 \cos\omega t)$, where C_{μ_0} and ϵ_2 are constants, and the outer flow is independent of time [$\epsilon_1 = 0$ in Eq. (19)]. Again, the foremost position of the separation point of the wall jet calculated by the unsteady method is very close to that calculated by the quasi-steady-state method. Similar results are obtained for calculations with different combinations of outer flow conditions, jet blowing rates, and slot locations. Based on the previous results, it is assumed that the separation point of the wall jet on the circulation-control airfoil can be calculated approximately by quasi-steady-state boundary-layer calculation.

For the boundary layer on the lower surface of the airfoil, quasi-steady-state approximation is also made. The boundary layer on the lower surface begins at the forward stagnation point with Heimenz stagnation-flow solution. Thwaites' method (Ref. 12, p. 108) is used to calculate the laminar boundary-layer development downstream of the stagnation point. The procedure of Granville[16] is used to predict transition. The turbulent boundary-layer development is calculated using Head's method (Ref. 12, p. 193).

Calculation Procedure

In this paper, the unsteady calculation starts from the steady-state condition, the steady flow around the airfoil under given flight conditions, and jet blowing rate is calculated as follows:

1) The separation point on the upper surface z_{10} is prescribed (Fig. 6).

2) Guess a separation point of the lower boundary layer, z'_{20}.

3) Potential flow is calculated with $U + iV$ independent of time and $\dot{\alpha} = 0$; nascent vortices are introduced near z_{10} and z'_{20} at each time step. The calculation is stopped when a steady state is approximately reached.

4) With the potential flow from step 3, the development of boundary layer on the lower surface is calculated. A new separation point, denoted as z_{20}, is obtained.

5) If z_{20} is significantly different from z'_{20}, z'_{20} is replaced by z_{20} and steps 3–4 are repeated. The above process is continued until z_{20} is not significantly different from the previous one.

6) Calculate the development of the wall jet starting from the slot. Keep adjusting the jet blowing rate until it separates at z_{10}.

The unsteady flow is calculated by the following procedure:

1) Assume that at time $t < 0$, the airfoil is moving with constant velocity and the blowing rate is constant; the separation points on the upper and lower surface and the potential flow are determined by the steady-state calculation procedure described above.

2) At time $t = 0$, the airfoil is set into translational and pitching oscillations and/or the jet blowing rate begins to oscillate. At each time step, the potential flow and boundary layer calculations are conducted consecutively. The calculation is carried on until the transient has faded and the response is repeatable (in our calculation, it was found that after two or three cycles, the response became periodical).

Results and Discussion

The calculation method has been applied to an elliptical circulation-control airfoil of 20% thickness ratio. First, the steady-state case is considered. An example is shown in Fig. 7, where the calculated and measured pressure distribution on the airfoil are compared. Good agreement is obtained except near the trailing edge of the airfoil. The measured peak pressure on the upper surface near the trailing edge of the airfoil is primarily due to the wall-jet entrainment effects, which is

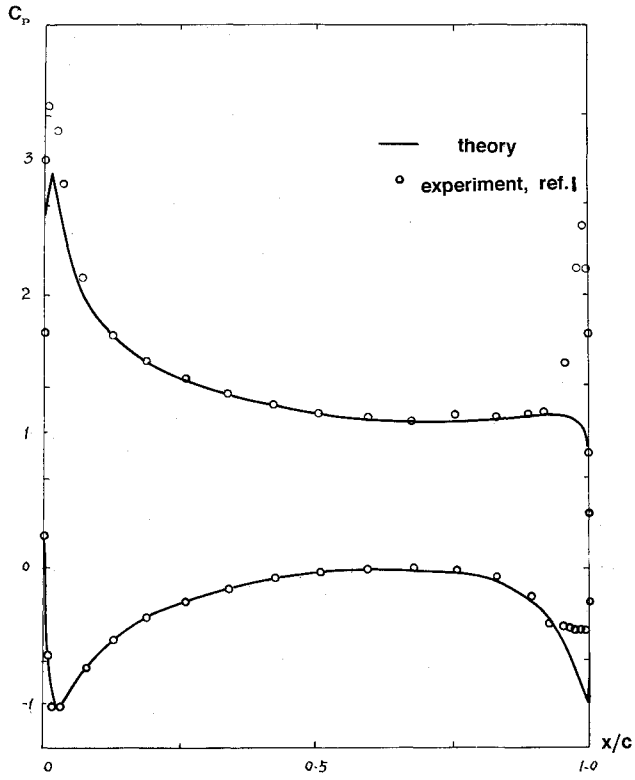

Fig. 7 Pressure distribution on circulation-control airfoil in steady state ($b/a = 0.2$; $C_\mu = 0.025$; and $\alpha = 4.4$ deg).

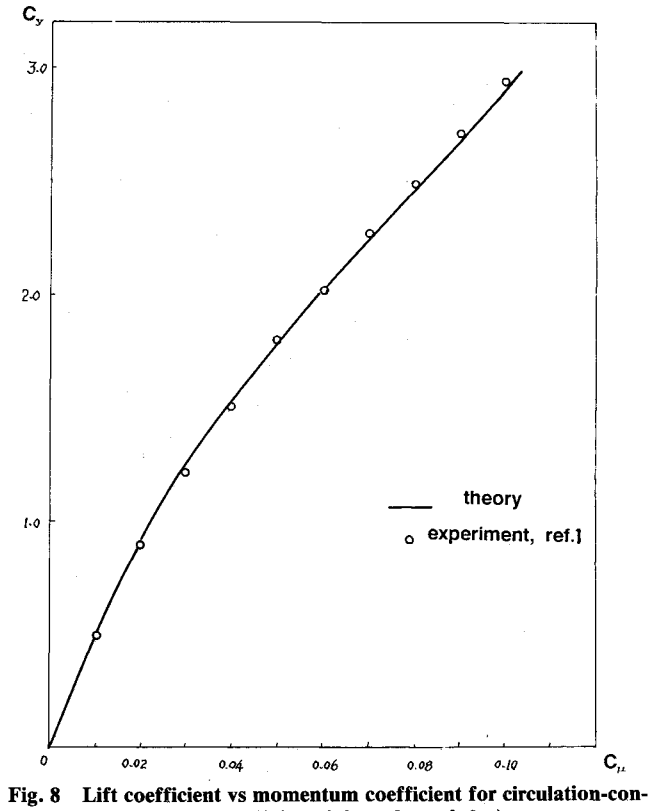

Fig. 8 Lift coefficient vs momentum coefficient for circulation-control airfoil in steady state ($b/a = 0.2$; and $\alpha = 0$ deg).

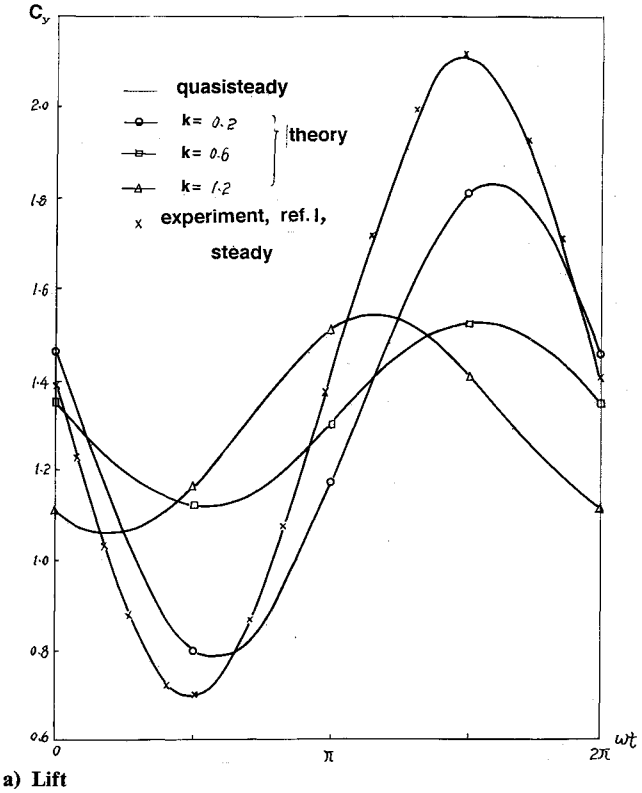

a) Lift

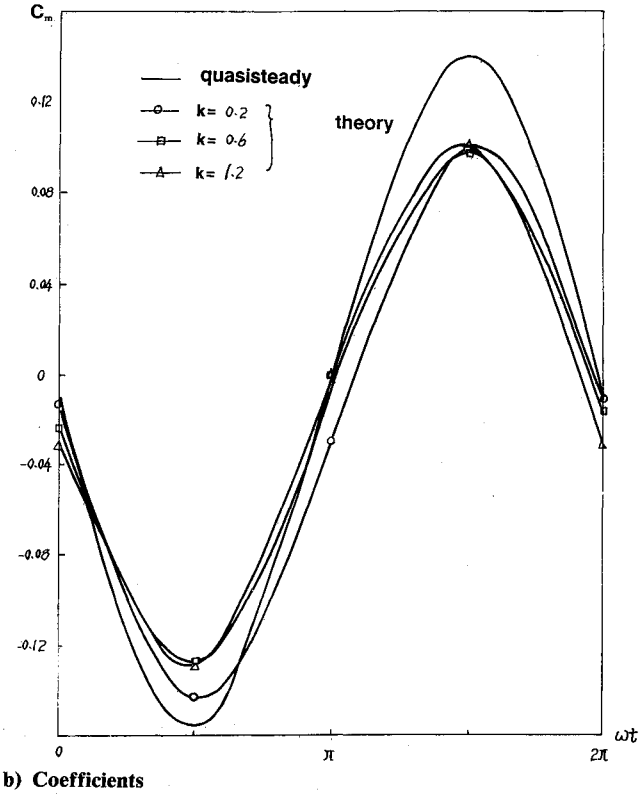

b) Coefficients

Fig. 9 Lift and moment coefficients for circulation-control airfoil vs time ($b/a = 0.2$; $U = 30$ m/s; $V = 0.1U_\infty \sin\omega t$; $\dot{\alpha} = 0$ deg; and $C_\mu = 0.035$).

not included in the present method. The pressure peak is in a very narrow region. Therefore, it will not have a large contribution to the lift of the airfoil, but it may have a large effect on the moment of the airfoil. Figure 8 shows the calculated lift coefficient as a function of the jet-momentum coefficient for the same airfoil. The experimental results are also presented. The lift calculation is in good agreement with the experiment. These correlations between theory and experiment also show that the discrete vortex method can calculate the steady-state potential flow with wake effects very well.

Next, some results of the unsteady calculation are described. Figure 9 shows the lift and moment coefficients as

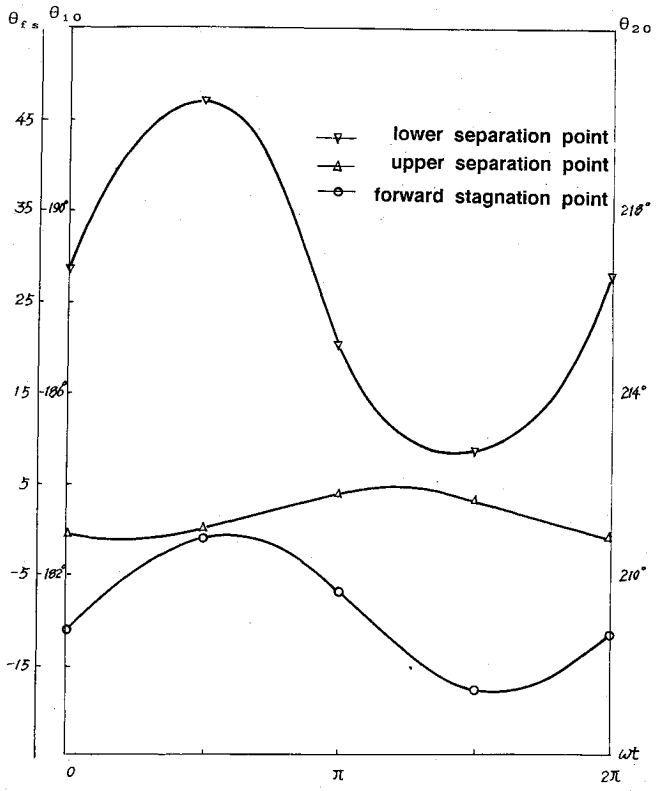

Fig. 10 Forward stagnation point and upper and lower separation points vs time ($k = 0.2$, other conditions are the same as in Fig. 9).

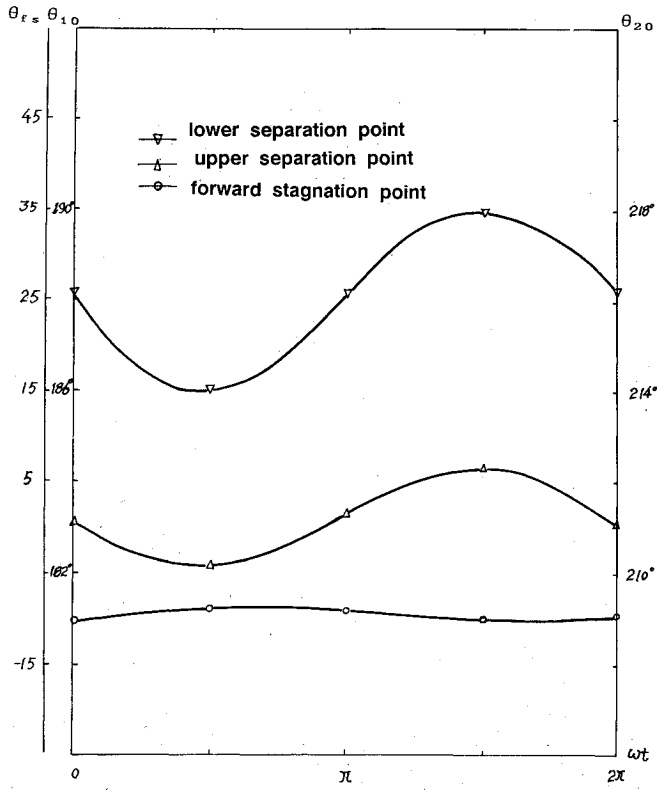

Fig. 12 Forward stagnation point and upper and lower separation points vs time ($k = 0.2$, other conditions are the same as in Fig. 11).

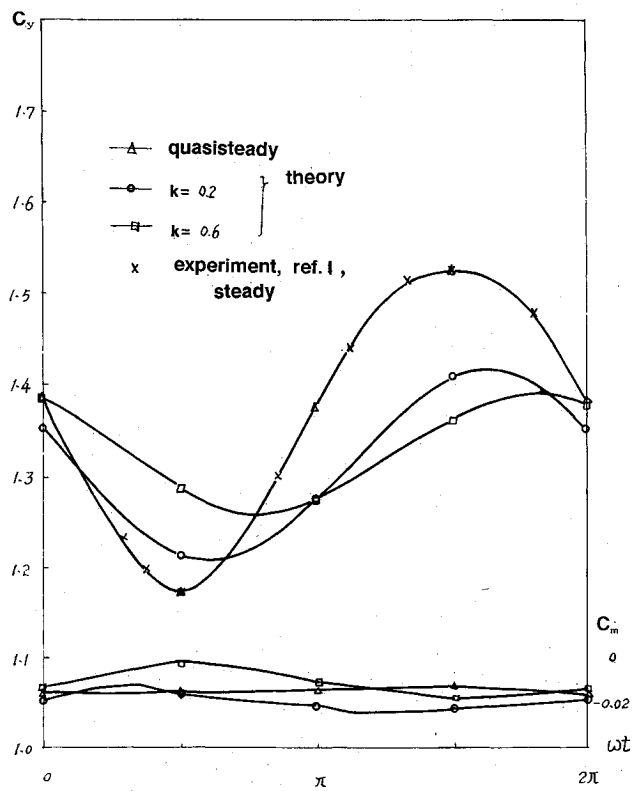

Fig. 11 Lift and moment coefficients for circulation-control airfoil vs time ($b/a = 0.2$; $U = 30$ m/s; $V = 0$; $\dot{\alpha} = 0$ deg; $C_\mu = C_{\mu 0}(1 - 0.2 \sin\omega t)$; and $C_{\mu 0} = 0.035$).

functions of time for different frequencies when the airfoil performs heave oscillations. Only steady-state experimental data for lift coefficients are available for comparison with the quasisteady calculation result. For this case, the agreement between the theory and experiment is good. From Fig. 9a, it is seen that as the frequency increases, the phase difference between the airfoil motion and the response increases first, and then decreases, and the amplitude of the response decreases first and then increases. The decrease of the phase difference and the increase of the amplitude at higher frequencies are due to the apparent mass force. The airfoil performs simple harmonic heave motion, but the response is not simple harmonic because of the nonlinearity of the problem. The time variations of the forward stagnation position and the upper and lower separation points corresponding to the case of $k = 0.2$ in Fig. 9 are shown in Fig. 10, The lower-surface separation point moves in a much larger range (from $\theta_{20} = 212.5$ to 220.5) than the upper-surface separation point; i.e., the separation point of the wall jet (from $\theta_{10} = 183$ to 184). This shows that the separation position of a boundary layer is more easily affected by outer flow variation than that of a wall jet. The interaction between the lower-surface boundary layer and the outer flow plays an important role in determining the aerodynamic forces on a circulation-control airfoil (with blowing jet on upper surface).

Figure 11 shows the lift and moment coefficients as functions of time for different frequencies when the jet-momentum coefficient varies sinusoidally and the airfoil moves at constant velocity. For the quasi-steady-state case, the calculated lift coefficient is compared with available experimental data and they are in good agreement. As the frequency is increased, the phase lag of the lift response will increase and the amplitude of the lift response will decrease. Figure 12 shows the time variations of the forward stagnation position and the upper and lower separation points corresponding to the case of $k = 0.2$ in Fig. 11. Again, it is seen that the amplitude of the oscillating lower-surface separation point is large.

From the results for heave motion and C_μ variation, it is seen that the unsteady aerodynamic force and moment response of the circulation-control airfoil is significantly different from that of the quasi-steady-state case. Therefore, it is necessary to use an unsteady flow model in the analysis of

aeroelasticity stability problems of circulation-control wings and blades.

Conclusions

A method for calculating unsteady flow of an elliptical circulation-control airfoil in an incompressible flow is developed. The following conclusions are made from this study:

1) Experimental correlations for steady flow show that combining the boundary-layer theory and the discrete vortex method can calculate the potential flow including wake effects with good accuracy. For accurate calculation of pressure distribution near the trailing edge, the wall-jet entrainment effects need to be included.

2) When the airfoil is performing simple harmonic heave oscillations, the lift response is periodic but not simple harmonic; as the reduced frequency increases, the lift amplitude decreases first and then increases, and the phase lag increases first and the decreases. The phase starts leading at high reduced frequencies.

3) When the jet-momentum coefficient varies sinusoidally, the lift response is periodic but not simple harmonic; the amplitude of the lift response decreases and the phase lag increases as the reduced frequency increases.

4) The interaction between the lower-surface boundary layer and the outer flow is important in determining the unsteady aerodynamic forces on a circulation-control airfoil.

References

[1]Kind, R. J., "A Proposed Method of Circulation Control," Ph.D. Thesis, Univ. of Cambridge, UK, June 1967.

[2]Englar, R. F. and Trobaugh, L. A., "STOL Potential of the Circulation Control Wing for High-Performance Aircraft," *Journal of Aircraft,* Vol. 15, Nov. 1978, pp. 175–181.

[3]Wood, N. J. and Nielsen, J. N., "Circulation Control Airfoils As Applied to Rotary-Wing Aircraft," *Journal of Aircraft,* Vol. 23, Dec. 1986, pp. 865–875.

[4]Dvorak, F. A. and Kind, R. J., "Analysis Method for Viscous Flow Over Circulation Control Airfoils," *Journal of Aircraft,* Vol. 16, June 1979, pp. 23–28.

[5]Sun, M., Pai, S. I., and Chopra, I., "Aerodynamic Force Calculation of an Elliptical Circulation Control," *Journal of Aircraft,* Vol. 23, Sept. 1986, pp. 673–680.

[6]Raghavan, V., Pai, S. I., and Chopra, I., "Circulation Control Airfoils in Unsteady Flow," 43rd Annual Forum and Technology Display of the American Helicopter Society, St. Louis, MO, May 1987.

[7]Milne-Thomson, L. M., *Theoretical Hydrodynamics,* 4th ed., MacMillan, New York, 1960, p. 251.

[8]Fagye, A. and Johansen, F. C., "The Structure of the Vortex Sheet," *Philosophical Magazine,* Vol. 7, 1928, pp. 417–436.

[9]Williams, J. C., "Incompressible Boundary-Layer Separation," *Annual Review of Fluid Mechanics,* Vol. 9, 1977, pp. 113–144.

[10]Sarpkaya, T. and Schoaff, R. L., "Inviscid Method of Two-Dimensional Vortex Shedding by a Circular Cylinder," *AIAA Journal,* Vol. 17, Nov. 1979, pp. 1193–1200.

[11]Stansby, P. K. and Dixon, A. G., "The Importance of Secondary-Shedding in Two-Dimensional Wake Formation at Very High Reynolds Numbers," *Aeronautical Quarterly,* May 1982, pp. 105–123.

[12]Cebeci, T. and Bradshaw, P., *Momentum Transfer in Boundary Layers,* Hemisphere, Washington, 1977.

[13]Dvorak, F. A., "Calculation of Turbulent Boundary Layers and Wall Jet Over Curved Surfaces," *AIAA Journal,* Vol. 11, 1973, pp. 517–524.

[14]Patel, R. P., "Self-Preserving, Two-Dimensional Turbulent Jets and Wall Jets in a Moving Stream," M.S.E. Thesis, Dept. of Mechanical Engineering, McGill Univ., Montreal, Canada, 1962.

[15]Bradshaw, P. and Gee, M. T., "Turbulent Wall Jet With and Without an External Stream," ARC, RM 3252, 1960.

[16]Granville, P. S., "The Calculation of Viscous Drag of Bodies of Revolution," David Talor Model Basin, Rept. 849, 1953.